Structural Characterization by Low Energy Auger Electron and Photoelectron Scattering

Y. U. Idzerda and D. E. Ramaker
Naval Research Laboratory, Washington, D.C. 20375
(Received 18 March 1992)

The angle-resolved electron intensity patterns of low energy Auger electrons and photoelectrons are calculated using a quantum mechanical electron scattering formalism with the inclusion of appropriate electron angular momentum. Calculations indicate that scattering of high angular momentum and low energy electrons exhibit minima in the forward direction whereas low angular momenta or high energy electrons exhibit maxima, as is experimentally observed. Comparison of experimental and theoretical patterns allows for detailed structural characterizations.

PACS numbers: 61.14.Rq, 61.14.Dc

Energy- and angle-resolved electron intensity distributions have been successfully used in recent years for the complete structural characterization of single-crystal films, overlayers, and surfaces [1-5]. Structural parameters can be extracted using various methodologies including fixed emission-direction electron spectroscopy [2] and fixed-energy, angle-dependent electron intensity mapping [3-5]. The experimental spectra of these proven techniques can be accurately reproduced by quantum mechanical electron scattering theories for relatively high energy (>200 eV) electrons [1-4]. These complete angular intensity mappings can be successfully Fourier transformed under appropriate constraints to form electron holograms [6-9]. Although the analysis of high energy electron scattering is well understood, major difficulties are found to arise when lower energy electrons are used.

In mapping the intensity of low energy Auger electrons for a variety of different materials, Frank *et al.* [10] found angular distributions which conflicted with the intuitive picture utilized for the scattering of higher energy electrons and obtained from the current quantum mechanical electron scattering formalism [1,11]. In this widely accepted picture, the angle-dependent variations of the emitted electron intensity are dominated by large electron intensity enhancements due to forward scattering of the electron wave as it traverses nearby atomic potentials. Instead of the expected intensity maxima, Frank *et al.* found intensity minima. To describe these minima, they proposed a physical model utilizing a more classical approach of attenuation of the emitted Auger electron. In this "blocking" model, atoms lying between the detector and the atomic site of the Auger emission block transmission of the Auger electron.

The mechanism underpinning this model was counter to the widely accepted forward scattering picture, producing strong objections to this "blocking" picture [12]. To investigate this apparent controversy, Terminello and Barton [13] examined isoenergetic Auger electrons and photoelectrons in an attempt to isolate the source of the phenomenon observed by Frank *et al.* Complete angular distribution patterns (ADPs) of the $M_{23}M_{45}M_{45}$ Auger electron intensities taken from the Cu(001) surface were compared to similar patterns for Cu $3p_{3/2}$ photoelectrons of the same energy (56.6 eV). Interestingly, they found that the Auger electron and photoelectron patterns were strikingly different: The Auger emission showed intensity minima along major crystalline directions, the photoelectron emission showed intensity maxima. They therefore concluded that electron scattering alone could be eliminated as the source of the differences, unless different final states resulting from the different emission processes played some crucial role (in particular, they speculated, if Auger emission is dominated by electrons with $l=2$, d character).

We show in this work that the features observed in the full angle-dependent intensity profiles can be generated by the basic electron scattering formalism, which has been used so successfully in the past, but care must be taken to include the final-state angular momentum of the emitted electron. Our calculational scheme is a single scattering cluster method [1,14] with the inclusion of spherical wave corrections [15]. We use the Rehr-Albers formalism [14] which is a general electron scattering formalism beginning with the separable free-electron Green's-function propagator. This formalism has been encoded by Friedman and Fadley [16] for monoenergetic, single scattering calculations.

The most insightful conclusions can be derived from a calculation of the angle-dependent intensity map for emission from Cu(001) to Pt(111). In Figs. 1(a) and 1(b) we compare the 56.6-eV $3p_{3/2}$ photoelectron angle-dependent profile (where both $l=0$ and $l=2$ final-state momenta contribute equally) with the calculated 56.6-eV, $M_3M_{45}M_{45}$ Auger electron profile (where we determine the dominant final-state angular momentum l to be 3). For the Auger transition, all the $2l+1$ final-state magnetic sublevels are equally populated ($m=+3$ to -3 for $l=3$ emission). The photoemission selection rules dictate that only the magnetic sublevels for $m=-1$ to $+1$ for the $l=2$ Cu $3p$ photoemission are included in the calculated intensity distribution. For these calculations, the unpolarized photons are represented by two polarization vectors, one along the detector direction and one orthogo-

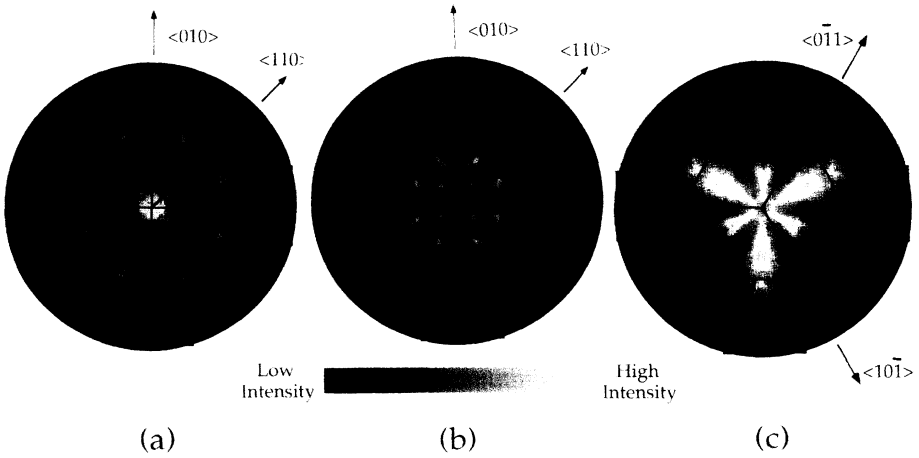

FIG. 1. Calculated angle-dependent electron intensity profiles for (a) Cu $3p$ photoemission (56.6 eV) from Cu(001) with emitted electron angular momentum $l=0$ and 2, (b) $M_3M_{45}M_{45}$ Cu Auger emission (56.6 eV) from Cu(001) with $l=3$, and (c) $N_{67}O_{45}O_{45}$ Pt Auger emission (65 eV) from Pt(111) with $l=3$. The color scale is reversed from Ref. [13] (bright is high intensity). The polar angle (0°-90°) is measured outward from the figure center (which corresponds to normal emission) and the azimuthal angle (0°-360°) is measured around the figure perimeter. Sample orientation is indicated by the arrows which represent crystalline directions.

nal and within the surface plane. The inclusion of the appropriate angular momentum character of the electron emission reproduces the striking differences observed by Terminello and Barton. Whereas emission of a Cu $3p$ photoelectron ($l=0$ and 2) produces intensity maxima, emission of an Auger electron ($l=3$) produces energy minima. As has been suggested earlier [16,17], it is the combination of high angular momentum, low energy, and small atomic distances which create reduced electron intensities in the direction of forward scattering.

Determination of the outgoing angular momentum for the Auger process can be made by examining the relative occupation of the allowed multiplets present in the Auger emission. The multiplets for the Cu $M_3M_{45}M_{45}$ ($3p3d3d$) transition include the following: $^1G(3,5)$, $^3F(3)$, $^1D(1,3)$, $^3P(1)$, and $^1S(1)$ where the possible l values of the emitted electron are indicated in the parentheses. The ^1G and ^3F multiplets dominate, giving nearly 90% of the total intensity, and these multiplets are almost all exclusively $l=3$ [18]. In contrast the Pt $N_{67}O_{45}O_{45}$ ($4f5d5d$) Auger transitions have the multiplets $^1G(1,3,5,7)$, $^3F(1,3,5)$, $^1D(1,3,5)$, $^3F(3)$, and $^1S(3)$. In this case the multiplet intensities are more balanced [19] because all multiplets contain $l=3$, and $l=3$ still dominates. Utilizing the proper radial matrix elements [18] and expressions derived by Cherkendorff [20], we find that $l=3$, electrons with f character, contributes over 95% of the intensity for the Cu, and ~90% for the Pt, with $l=1$ dominating the small remainder.

It should be noted that hole-hole correlation effects present in the Auger process cannot alter the various angular momentum contributions which we have calculated. Within the final-state rule for Auger line shapes [21], it is the initial state which determines the total contribution of each component of the Auger intensities, while the final state determines the spectral distribution of each component. Thus, no redistribution of angular momentum values occurs and we expect electron blocking for high electron angular momenta regardless of the localization of the Auger final state.

The value of the electron scattering formalism is that it can predict the experimental results. In general, good agreement is obtained between our calculated Cu Auger angle-dependent map from Cu(001), the measured photon-stimulated Cu Auger mapping of Terminello and Barton, as well as with the electron-stimulated Cu Auger mapping of Frank *et al.* [22]. Not only do the intensity minima for electron emission lie perpendicular to the surface, but details of the intensity maxima are reproduced. In Fig. 1 we have not included the effects of the in-plane linear polarization of the photons generated by the synchrotron, multiple scattering effects, or the possibility of anisotropic population of the magnetic sublevels. Including multiple scattering might improve the quantitative agreement, but the position of minima and maxima should be unchanged [23].

The Pt(111) surface is another system which has been experimentally mapped using low energy (65 eV) $N_{67}O_{45}O_{45}$ Pt Auger electrons. We have modeled the emission from Pt(111) using only $l=3$ final-state angular momentum which dominates. The resultant profile, shown in Fig. 1(c), shows intensity minima along neighbor atomic directions in agreement with observed Pt Auger intensity profiles [10]. Similar agreement between experimental and single scattering cluster theory has been obtained very recently by Gerber *et al.* [24] for low ener-

gy *LVV* Al Auger emission where the contributions of the *s*, *p*, and *d* character of the Auger emission are extracted from the data.

To illustrate the mechanism which generates the strong variations in forward scattering intensities, a refinement to the intuitive picture for electron scattering must include the angular momentum dependence of the scattered electron. To include the effect on the scattering by the electron angular momentum, the atomic potentials can be represented by an effective potential which incorporates the attractive screened Coulomb potential with a repulsive centrifugal potential. The repulsive potential can be described by an effective or average angular momentum value, which is determined from a suitable partial-wave decomposition of the incident electron in terms of the spherical harmonics of the nearby scattering potential and depends on the electron angular momentum, the electron energy, and the atomic spacing. The range and strength of the centrifugal barrier increase as the angular momentum of the scattering electron is increased [25]. This is not a rigorous description of the scattering potential, nor does it describe the actual scattering calculation, but it is a useful construction to illustrate the mechanism which leads to the intensity enhancements and reductions.

The additional centrifugal potential affects the electron scattering in two ways. For electrons with large angular momentum, the combined effective potential develops a significant repulsive barrier outside the attractive well. Low energy electrons traversing the outer regions of the atomic potential are repelled by the repulsive barrier before being focused by the inner attractive well. The resulting scattering leads to a decreased intensity in the forward direction. At slightly higher energies, the electrons can penetrate the outer barrier and be forward focused by the inner attractive well. At energies of a few hundred eV, the electrons are nearly unaffected by the small repulsive barrier and only interact with the strong attractive well, resulting in large forward scattering intensities. Second, because the electron wave function is complex, the centrifugal barrier generates an additional phase shift for the scattered wave which can result in destructive interference [26]. Our calculations show that both the scattered intensity and accumulated phase are important in defining the intensity mappings.

Although these calculations reproduce the salient features of the simple classical picture of atomic blocking proposed by Frank *et al.* [10], several significant discrepancies remain. Contrary to the blocking model, reduced forward scattering intensities do not occur for all low energy Auger electrons. Only Auger processes which result in outgoing electrons of high angular momentum will have a significant outer centrifugal barrier. Also, strong high-order diffraction of the low energy electrons, which is inherently present in our calculations, can result in intensity features which simple atomic blocking fails to predict [e.g., no intensity minima along the ⟨011⟩ directions of the Cu(001) Auger pattern]. At higher energies, forward scattering enhancements are always present and no analogy with the blocking model is present. This final point is most clearly seen in the modeling of the 357-eV Ag Auger electron angular profiles for two monolayers of Ag on Pt(111) (see Fig. 2) as well as individual monolayers of I/Ag/Pt(111) (not shown). (For Ag Auger emission, we calculate $l=2$ is dominant in the electron emission.) The best agreement between experiment and the electron scattering formalism is obtained when the Ag

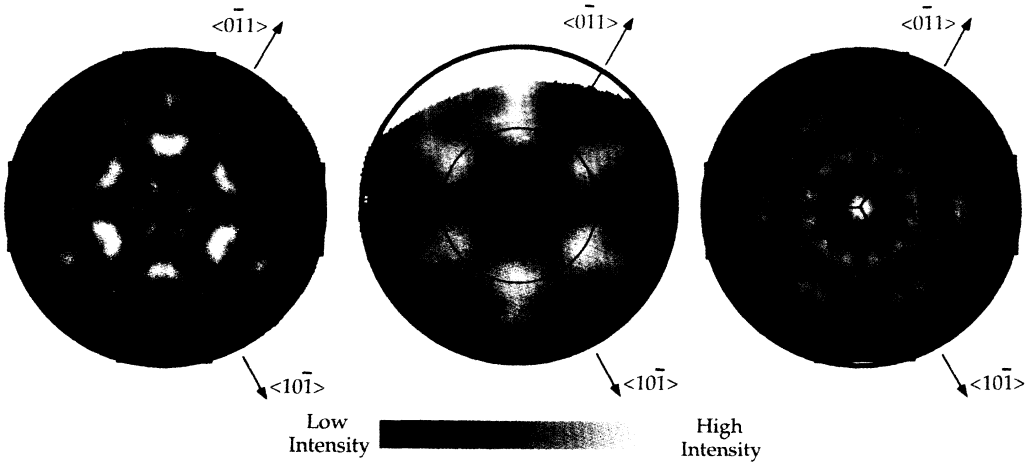

FIG. 2. Angle-dependent electron intensity profiles for 357-eV Auger emission from 2 ML Ag/Pt(111). Left: Calculated profile with $l=2$ for 2 ML Ag/7 ML Pt(111), Ag atoms all in threefold hollow sites (two domains equally represented). Center: Experimental intensity profile (from Ref. [27]). Right: Calculated profile with $l=2$ for 2 ML Ag/7 ML Pt(111), Ag atoms in atop-atop sites (after Ref. [27]).

(or I) atoms equally occupy the two domains of the threefold hollow sites, fcc stacking and hcp stacking sites, instead of the unique atop-atop configuration suggested by the blocking model [27]. Similar conclusions were obtained by Hu and King [9] for the I/Ag/Pt(111) system modeled using only $l=0$ emission.

We are grateful for the use of the University of Washington EXAFS code [FEFF 3.0, see J. J. Rehr, J. Mustre de Leon, S. I. Zabinsky, and R. C. Albers, J. Am. Chem. Soc. **113**, 5135 (1991)] for generating our atomic potentials and to D. J. Friedman and C. S. Fadley for providing us with the general-purpose single scattering diffraction computer program used for these calculations. (For a description of the formalism, see Refs. [14] and [16].) We would also like to acknowledge useful discussions with C. S. Fadley and J. J. Rehr. The support of the Office of Naval Research is gratefully acknowledged.

[1] C. S. Fadley, Prog. Surf. Sci. **16**, 275 (1984); in *Synchrotron Radiation Research: Advances in Surface Science*, edited by R. Z. Bachrach (Plenum, New York, 1990), and references therein.

[2] J. J. Barton *et al.*, Phys. Rev. Lett. **51**, 272 (1983); J. J. Barton, C. C. Bahr, and D. A. Shirley, in *The Structure of Surfaces*, edited by M. A. Van Hove and S. Y. Tong (Springer-Verlag, Berlin, 1985).

[3] W. F. Egelhoff, Jr., Crit. Rev. Solid State Mat. Sci. **16**, 213 (1990).

[4] S. A. Chambers, Adv. Phys. **40**, 357 (1991).

[5] B. Maschoff, J.-M. Pan, and T. E. Madey, Surf. Sci. **259**, 190 (1991).

[6] J. J. Barton, Phys. Rev. Lett. **67**, 3106 (1991).

[7] S. Thevuthasau, G. S. Herman, A. P. Kaduwela, R. S. Saiki, Y. J. Kim, W. Niemczura, M. Burger, and C. S. Fadley, Phys. Rev. Lett. **67**, 469 (1991).

[8] G. K. Harp. D. K. Saldin, and B. P. Tonner, Phys. Rev. Lett. **65**, 1012 (1990).

[9] P. Hu and D. A. King, Nature (London) **353**, 831 (1991).

[10] D. G. Frank, N. Batina, T. Golden, F. Lu, and A. T. Hubbard; Science **247**, 182 (1990); D. G. Frank, N. Batina, J. W. McCargar, and A. T. Hubbard, Langmuir **5**, 1141 (1989).

[11] M. L. Xu, J. J. Barton, and M. A. Van Hove, Phys. Rev. B **39**, 8275 (1989); H. C. Poon and S. Y. Tong, Phys. Rev. B **30**, 6211 (1984).

[12] S. A. Chambers, Science **248**, 1129 (1990); W. F. Egelhoff, Jr., J. W. Gadzuk, C. J. Powell, and M. A. Van Hove, Science **248**, 1129 (1990); X. D. Wang, S. L. Han, B. P. Tonner, Y. Chen, and S. Y. Tong, Science **248**, 1129 (1990); D. P. Woodruff, Science **248**, 1131 (1990).

[13] L. J. Terminello and J. J. Barton, Science **251**, 1218 (1991).

[14] J. J. Rehr and R. C. Albers, Phys. Rev. B **41**, 8139 (1990).

[15] M. Sagurton, E. L. Bullock, R. Saiki, A. Kaduwela, C. R. Brundle, C. S. Fadley, and J. J. Rehr, Phys. Rev. B **33**, 2207 (1986).

[16] D. J. Friedman and C. S. Fadley, J. Electron. Spectrosc. Relat. Phenom. **51**, 689 (1990).

[17] R. N. Lindsey and C. G. Kinneburgh, Surf. Sci. **63**, 162 (1977).

[18] E. J. McGuire, Phys. Rev. A **16**, 2365 (1977); E. J. McGuire, Sandia National Laboratories Research Report No. SC-RR-71-0075, 1971 (unpublished); SC-RR-71-0835, 1972 (unpublished); SAND-75-0443, 1975 (unpublished).

[19] The individual multiplets have been experimentally resolved in the gas phase for the neighboring elements Hg and Au; H. Aksela, S. Aksela, J. S. Jen, and T. D. Thomas, Phys. Rev. A **15**, 985 (1977); S. Aksela, M. Harkoma, M. Pohjola, and H. Aksela, J. Phys. B **84**, 2227 (1984).

[20] I. Cherkendorff, J. Electron Spectrosc. Relat. Phenom. **32**, 1 (1983).

[21] D. E. Ramaker, Phys. Rev. B **25**, 7341 (1982).

[22] D. G. Frank, T. Golden, O. M. R. Chyan, and A. T. Hubbard, J. Vac. Sci. Technol. A **9**, 1254 (1991).

[23] M. L. Xu and M. A. Van Hove, Surf. Sci. **207**, 215 (1989).

[24] T. Greber, J. Osterwalder, S. Hufner, and L. Schlapbach, Phys. Rev. B **45**, 4540 (1992).

[25] Most important, the effective angular momentum and therefore the barrier height increase as the angular momentum of the emitted electron increases (see Ref. [14]).

[26] See D. P. Woodruff, Science **248**, 1131 (1990); also J. J. Rehr, R. C. Albers, C. R. Natoli, and E. A. Stern, Phys. Rev. B **34**, 4350 (1986).

[27] A. T. Hubbard, D. G. Frank, O. M. R. Chyan, and T. Golden, J. Vac. Sci. Technol. B **8**, 1329 (1990).

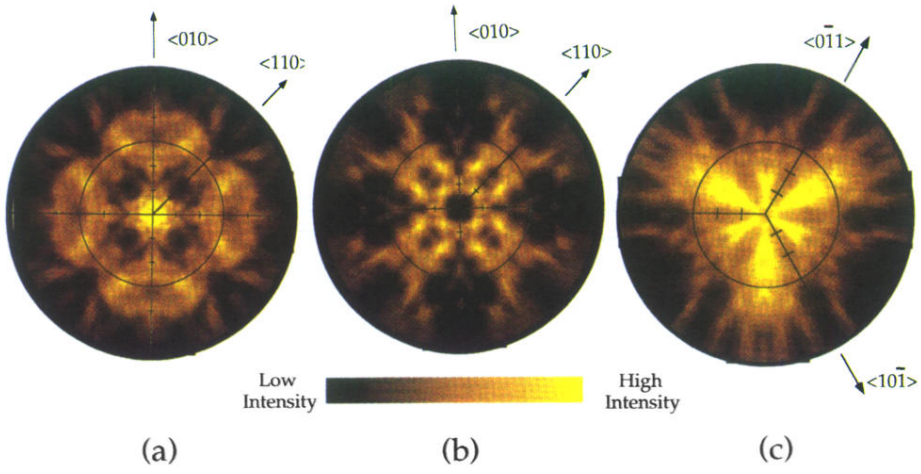

FIG. 1. Calculated angle-dependent electron intensity profiles for (a) Cu $3p$ photoemission (56.6 eV) from Cu(001) with emitted electron angular momentum $l=0$ and 2, (b) $M_3M_{45}M_{45}$ Cu Auger emission (56.6 eV) from Cu(001) with $l=3$, and (c) $N_{67}O_{45}O_{45}$ Pt Auger emission (65 eV) from Pt(111) with $l=3$. The color scale is reversed from Ref. [13] (bright is high intensity). The polar angle (0°–90°) is measured outward from the figure center (which corresponds to normal emission) and the azimuthal angle (0°–360°) is measured around the figure perimeter. Sample orientation is indicated by the arrows which represent crystalline directions.

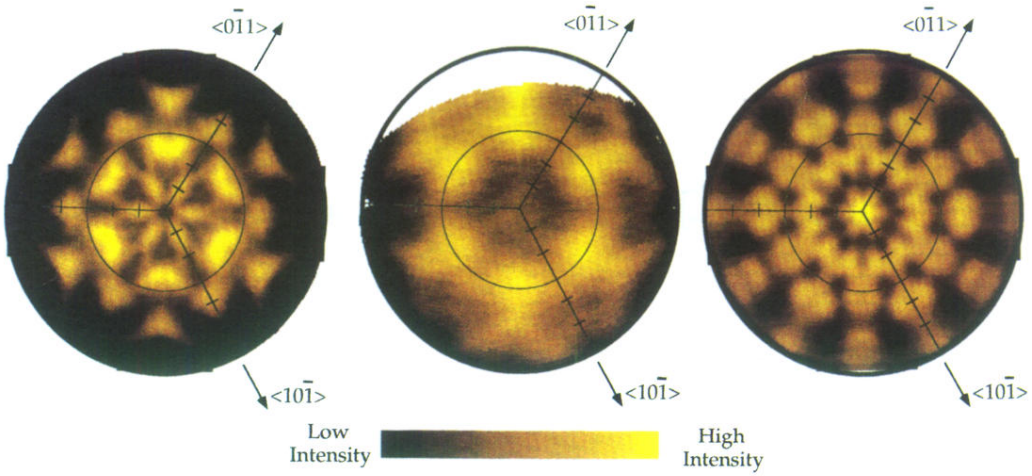

FIG. 2. Angle-dependent electron intensity profiles for 357-eV Auger emission from 2 ML Ag/Pt(111). Left: Calculated profile with $l=2$ for 2 ML Ag/7 ML Pt(111), Ag atoms all in threefold hollow sites (two domains equally represented). Center: Experimental intensity profile (from Ref. [27]). Right: Calculated profile with $l=2$ for 2 ML Ag/7 ML Pt(111), Ag atoms in atop-atop sites (after Ref. [27]).